

Nonlinear switching dynamics in a nanomechanical resonator

Quirin P. Unterreithmeier,^{*} Thomas Faust, and Jörg P. Kotthaus

Fakultät für Physik and Center for NanoScience (CeNS), Ludwig-Maximilians-Universität, Geschwister-Scholl-Platz 1,
D-80539 München, Germany

(Received 26 April 2010; published 7 June 2010)

We report studies on the nonadiabatic time evolution of a nonlinear resonator subject to short and intense resonant RF actuation. We are able to quantitatively model the experimental data using a Duffing oscillator. Applying suitably chosen RF pulses, we demonstrate active switching between the two stable states of a Duffing oscillator on short time scales, well below the relaxation time.

DOI: [10.1103/PhysRevB.81.241405](https://doi.org/10.1103/PhysRevB.81.241405)

PACS number(s): 85.85.+j, 05.45.-a, 62.25.-g

The oscillatory response of nonlinear systems exhibits characteristic phenomena such as multistability,¹ discontinuous jumps,^{2,3} and hysteresis.³ These can be utilized in applications leading, e.g., to precise frequency measurement,⁴ mixing,⁵ memory elements,^{6,7} reduced noise characteristics in an oscillator,⁸ or signal amplification.⁹⁻¹² Approaching the quantum regime,¹³ concepts have been proposed that enable low backaction measurement techniques¹¹ or facilitate the visualization of quantum mechanical effects.¹⁴

Nanoelectromechanical systems (NEMS) have been established as excellent devices to explore nonlinear dynamical behavior, as they exhibit high mechanical quality (Q) factors,^{15,16} fast response times,¹⁷ and fairly low drift,¹ and can be easily excited into the nonlinear regime.¹ Here we study the time-dependent response of NEMS resonators in the nonlinear regime aiming at a more detailed understanding of the dynamics. Complementary to previous investigations that concentrated on phenomena arising near the onset of bistability,^{1,4,9} we present experiments that yield insight into the time evolution of the mechanical system. As we apply strong pulses, the system moves away from a stationary state and we study its response to this nonadiabatic actuation. The system is thereby highly excited into the nonlinear regime up to ten times the critical amplitude. Please note that the influence of the actuation on the lattice temperature of the beam is negligible.⁴ We employ our extended knowledge to perform fast switchings between the stable states no longer bound by relaxation times.

The employed resonator consists of a doubly clamped silicon nitride string of dimensions $35\ \mu\text{m} \times 250\ \text{nm} \times 100\ \text{nm}$ (length, width, and height, respectively) under high tensile stress, leading to high mechanical Q factors.¹⁸ In vacuum and at room temperature, we electrically excite the resonator at RF frequencies employing dielectric gradient forces provided by suitably located and biased electrodes.^{18,19} Illuminating the resonator with a light emitting diode, we detect the resonant motion by a small on-chip Schottky diode fabricated close to the resonator and serving as a photodetector for the oscillating component of the optical near field as discussed in detail elsewhere.²⁰ As this scheme enables the detection of the resonator's Brownian motion at room temperature we are able to convert the measured signal into absolute displacement. The nonlinear resonator is continuously actuated by the RF output of a network analyzer as depicted in Fig. 1(a).

Applying sufficiently strong excitation amplitudes, the

mechanical response around resonance tends to bend toward higher frequencies as depicted in Fig. 1(b), corresponding to string hardening. This behavior can be quantitatively modeled by solving the so-called Duffing equation,²¹ an extension of the simple harmonic oscillator by a nonlinear term of third order.

$$\ddot{x}(t) + \frac{2\pi f_0}{Q}\dot{x}(t) + (2\pi f_0)^2 x(t) + \alpha_3 x(t)^3 = k \cos[2\pi(f_0 + \sigma)t]. \quad (1)$$

Here, $x(t)$ designates resonator displacement, $f_0=8$ MHz, $Q=1.2 \times 10^5$ its resonance frequency and quality factor; and α_3 is the cubic correction to the linear restoring force. The excitation amplitude is k and its frequency detuning from the mechanical resonance is $\sigma=f-f_0$. We apply a perturbation calculation using the ansatz $x(t)=a(t)\cos[2\pi(f_0+\sigma)t+\gamma(t)]$, with time-dependent displacement amplitude $a(t)$ and phase $\gamma(t)$. This leads to the two coupled equations²¹

$$\begin{aligned} \dot{a}(t) &= -\frac{2\pi f_0 a(t)}{2Q} + \frac{k \sin[\gamma(t)]}{4\pi f_0}, \\ \dot{\gamma}(t) &= 2\pi\sigma - \frac{3\alpha_3 a(t)^2}{16\pi f_0} + \frac{k \cos[\gamma(t)]}{4\pi f_0 a(t)}. \end{aligned} \quad (2)$$

By setting $\dot{a}(t)=0$, $\dot{\gamma}(t)=0$, one arrives at the quasistatic solution $a=a(f)$. This curve can be excellently fitted to the measured data [see Fig. 1(b)], thereby obtaining $\alpha_3=9 \times 10^{26}\ (\text{ms})^{-2}$ as the only additional numerically adjusted parameter. The onset of bistability, at which the first and second derivative of the amplitude with respect to f diverge [$\partial a/\partial f=\infty$, $\partial^2 a/(\partial f)^2=\infty$] is called critical displacement. Throughout this work, all displacements $a(t)$ are given in units normalized to this critical displacement, it applies $a_c=4\sqrt{2}\pi f_0/(3^{3/4}\sqrt{\alpha_3 Q})=6\ \text{nm}$ (half peak-to-peak), the corresponding critical actuation amplitude is $k_c=150\ \text{ms}^{-2}$.

Figure 1(c) shows the calculated displacement response of the resonator when actuated with an excitation amplitude that is ten times larger than the critical actuation leading to the critical displacement a_c . In the following, we always continuously excite our system $\sigma=1$ kHz above resonance, well in the bistable regime. The two stable oscillatory amplitudes are marked as blue dots in Fig. 1(c).

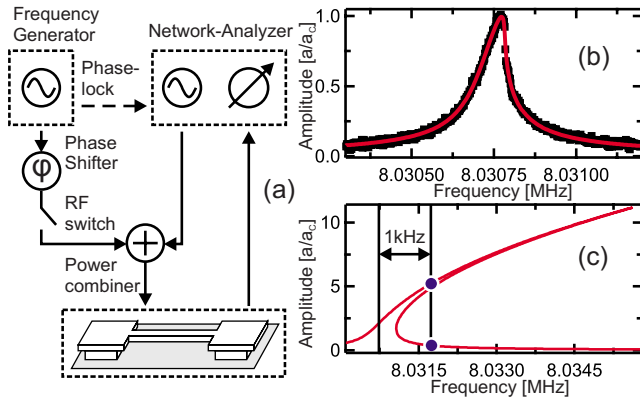


FIG. 1. (Color online) *Setup and quasistatic response*: (a) schematic setup, a nanomechanical resonator is continuously actuated in the nonlinear regime using the RF output of a network analyzer; additional RF pulses of the same frequency are provided by a frequency generator that is phase-locked to the network analyzer; the output of the frequency generator can be adjusted to any phase φ with respect to the continuous actuation; an RF switch defines short RF pulses. The resonator's oscillatory state, given by its displacement amplitude a and phase γ , is recorded by a nearby photodiode and the network analyzer. (b) Quasistatic response to continuous actuation near the onset of bistability, measurement (black) and fit (red/gray) using a solution of the Duffing equation; the displacement amplitude a is given in units of the critical displacement a_c , marking the onset of bistability. (c) Calculated response when actuating ten times the critical driving amplitude. At an actuation frequency f 1 kHz above resonance f_0 , two stable oscillation amplitudes exist, marked with blue/dark gray dots; this actuation is used for all following measurements.

To gain insight into the dynamical behavior of our system, we measure the relaxation toward one of these stable points of the continuously driven string after additional pulsed excitation. The pulsed excitation is provided by the output of a frequency generator that is phase-locked to the network analyzer and operates at the same frequency f as the continuous drive. The phase of the frequency generator's signal can be adjusted to any phase φ with respect to the continuous drive as sketched in Fig. 1(a). To avoid confusion, we always specify the two phases with their respective symbol γ or φ in the ongoing text. An RF switch serves to define RF pulses of adjustable duration.

Any nonstationary resonator state [defined by its displacement amplitude a and phase γ referred to the continuous drive; or equivalently by its in-phase $[a \cos(\gamma)]$ and out-of-phase $[a \sin(\gamma)]$ amplitude component] will converge toward either of the two stable states. This convergence divides the resonator's phase space into two basins of attraction,^{1,21} as depicted in Fig. 2(a) as black and white regions, obtained by numerically integrating Eqs. (2). To test this simulated behavior experimentally, we apply the described short and intense RF pulse that excites the oscillator away from the stable state. Immediately after switching off this pulse, we start recording the resonator state with a sampling rate of 100 kHz. Depending on amplitude, duration, and phase φ of the pulsed excitation, the resonator's dynamic state starts in either the white or black region of phase space directly after excitation and relaxes in a spiraling motion toward either of

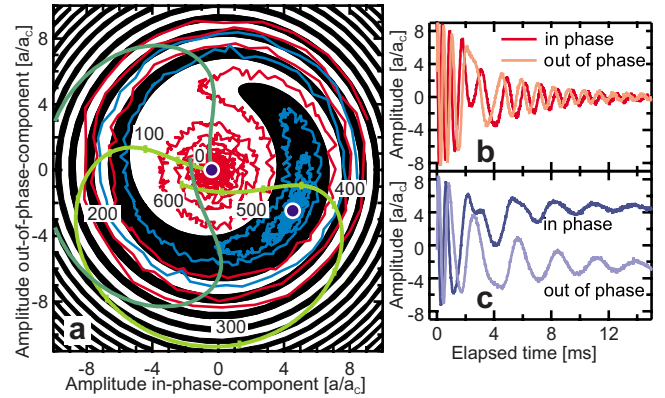


FIG. 2. (Color online) *Time evolution of the resonator state*: (a) the resonator's phase space is shown parametrized by the in $[a \cos(\gamma)]$ and out-of-phase $[a \sin(\gamma)]$ components of the oscillatory displacement. Because of the nonlinear actuation, two stable points exist (blue/dark gray dots), each having its (calculated) basin of attraction (black/white: high/low displacement amplitude). The displayed traces (red/gray and blue/dark gray lines) show the measured relaxation of an oscillatory state after being excited to an amplitude $a \approx 8a_c$ for two different excitation phase φ settings. (b) and (c) display the same relaxation process versus time, the trace color corresponds to (a). The smooth green curves in a show the calculated time evolution during the application of an RF pulse of phases $\varphi = 262^\circ$, 172° (light and dark curve, respectively) and an amplitude 18-fold larger than the continuous actuation starting from the lower stable state; the displayed time values are given in μs .

the stable states staying within the respective region of phase space as theoretically predicted. In Fig. 2(a) two measured traces of such a relaxation differing in the phase φ of the previously applied RF pulse are plotted in phase space and show excellent agreement with theory. Figures 2(b) and 2(c) display the evolution with time, showing fast dynamics for high amplitudes. Eventually, the state oscillates around either of the stable points with constant frequency.

We intend to utilize the pulses to controllably switch between the stable points, therefore we apply an indirect measurement scheme to explore the nonadiabatic time evolution during strong pulse excitation. Such an indirect scheme is needed because electric crosstalk prevents a direct measurement of the resonator's state during the strong RF pulses. To predict the action of the RF pulse excitation in addition to the continuous drive, the green curves shown in Fig. 2(a) display the calculated mechanical response to a pulse excitation amplitude of $k_{\text{Pulse}} \approx 27 \times 10^3 \text{ ms}^{-2}$ corresponding to 18 times the continuous drive. Both curves start in the lower stable state, they differ in the phase φ of the applied pulse and are obtained by numerically time integrating Eqs. (2). As can be inferred from Fig. 2(a), we consecutively cross the two basins of attraction. Thereby, any resonator state with an amplitude lower than $\approx 10a_c$ can be addressed by suitably choosing the pulse phase and duration with the given pulse amplitude.

In the experiment, the oscillator is prepared in its lower stable state by subsequently switching off and on the continuous actuation. We then apply a short RF pulse with the same excitation amplitude as in the above calculation. After

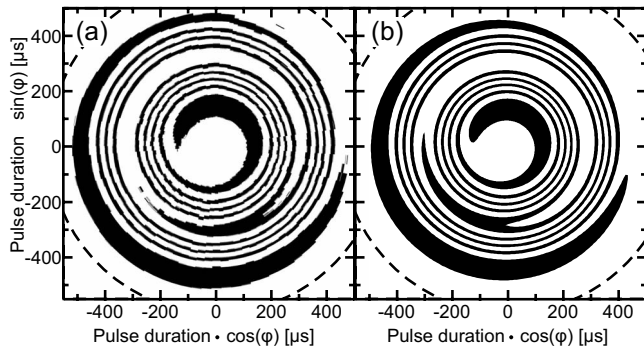


FIG. 3. Time evolution during the application of an RF pulse: (a) measured final state (black/white: high/low displacement amplitude) after the application of RF pulses causing a nonadiabatic response as shown in Fig. 2, systematically varied in duration and phase φ and plotted in polar coordinates. (b) Simulation of the measurement employing no fit parameters.

waiting several relaxation times given by $Q/(2\pi f_0)$, the attained stable state is recorded in displacement amplitude a and phase γ . We repeat this sequence, restore the lower stable state and systematically vary the length of the RF pulse and its phase φ ; the excitation amplitude is always the same. Thereby we implicitly map the end point of the green traces as shown in Fig. 2(a) and obtain the spirals in Fig. 3(a). This measured result is in excellent agreement with the calculation shown in Fig. 3(b), employing no fit parameters. The range of achieved displacement amplitudes extends those of previous measurements¹ to values of ten times the critical amplitude a_c . We can deduce that the perturbation solution describing the time evolution Eqs. (2) remains accurate at least up to displacements that correspond to ten times the critical amplitude a_c . This demonstrates that the dynamics of a strongly driven nanomechanical resonator can still be accurately described by a perturbation solution of the Duffing equation, therefore serving as model system to study nonlinear dynamics^{22,23} well in the nonadiabatic regime.

Our quantitative understanding of the experiment enables us to numerically calculate the parameters needed in order to access any desired resonator state. In particular we are able to switch directly between the two stable states. We thus extend previous concepts^{6,7} of switching limited by the relaxation time scale $Q/(2\pi f_0)$ to active switching via RF pulses suitably chosen in amplitude, phase, and length. Figure 4(a) shows two consecutive switching events; during the 80- μ s-long RF pulses electric crosstalk produces overshoots partially exceeding the displayed range of displacement amplitudes. The nearly constant amplitude values highlighted by gray areas reflect the respective stable state of the bistable system. Note that the approach toward these constant amplitudes occurs on a time scale of less than 1 ms and only reflects the limited dynamics of the electronic measurement setup in contrast to the mechanical relaxation behavior studied in Figs. 2(b) and 2(c).

Since we can pulse toward either of the targeted stable states with high precision in phase space, we can switch between the stable states with a high repetition rate. Any systematic deviation would add up, eventually preventing controllable switching. Figure 4(b) shows ten consecutive

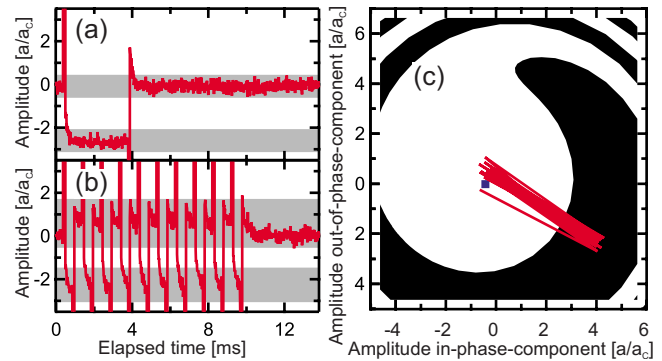


FIG. 4. (Color online) Switching between the stable points: (a) Out-of-phase component of the measured resonator displacement $a \sin(\gamma)$; the part of nearly constant amplitude (highlighted by the gray background) corresponds to the stable points; the spikes are a result of electric crosstalk when applying short RF pulses suitably chosen to directly switch between these states and do not correspond to displacement amplitudes. (b) Consecutive switching; ten pairs of switching events are shown; the duration of one pulse is approximately 80 μ s, the repetition rate of the pairs is 1 kHz. Because of the finite measurement bandwidth and electric crosstalk there is a systematic deviation compared to (a). (c) The same measurement displayed in phase space.

switching events within ten milliseconds each going back and forth between the two stable states. This corresponds to a demonstrated operating speed of 2 kHz. The applied pulse duration of 80 μ s of a single pulse allows operation speeds of approximately 11 kHz. In Fig. 4(c), we plot the same switching sequence in phase space. The image shows some systematic deviation of the measured traces with respect to the predicted stable states occurring immediately after the application of an RF pulse. This deviation is a result of the electric crosstalk and the finite bandwidth of the measurement setup. The experimentally chosen pulse durations deviate by less than 4% from the ones that were predicted theoretically.

The duration of the switching pulses corresponds here to approximately 1000 cycles of oscillation. This is significantly less than the number of oscillations required for the relaxation from an excited to a stable state corresponding to several times the quality factor of here $Q=1.2 \times 10^5$. Although being advantageous in terms of power consumption, a high-quality factor prevents fast switching in passive schemes, such as a sudden parameter change⁷ or the introduction of a weak external perturbation.⁶ Our scheme overcomes this limitation and achieves a four orders of magnitude improvement in speed when compared to these previous results.

It remains to be shown whether any logic or memory based on nanomechanical elements will play a significant role in the future. To achieve an operating speed of 100 MHz, another improvement of switching duration of 10^4 is required. As resonators with GHz resonance frequencies¹⁷ and high-quality factors¹⁶ have been demonstrated, this goal is not principally out of reach.

In conclusion, we quantitatively study the dynamical oscillatory response of a nonlinear nanomechanical resonator

in bistable configuration. The application of short RF pulses allows us to modify the resonator state at will. We utilize these pulses to highly excite the resonator. The measured results can be excellently modeled using a combination of perturbation calculation and numerical integration. We thereby directly confirm the accuracy of this model calculation to describe nonlinear dynamics.^{14,23} Our quantitative understanding allows us to predict and generate RF pulse

parameters that directly switch between the two stable states repeatedly.

Financial support by the Deutsche Forschungsgemeinschaft under Project No. Ko 416/18 as well as the German Excellence Initiative via the Nanosystems Initiative Munich (NIM) and LMUexcellent is gratefully acknowledged. We thank E. M. Weig for critically reading the manuscript.

*quirin.unterreithmeier@physik.uni-muenchen.de

- ¹I. Kozinsky, H. W. C. Postma, O. Kogan, A. Husain, and M. L. Roukes, *Phys. Rev. Lett.* **99**, 207201 (2007).
- ²W. J. Venstra and H. S. J. van der Zant, *Appl. Phys. Lett.* **93**, 234106 (2008).
- ³G. Gabrielse, H. Dehmelt, and W. Kells, *Phys. Rev. Lett.* **54**, 537 (1985).
- ⁴J. S. Aldridge and A. N. Cleland, *Phys. Rev. Lett.* **94**, 156403 (2005).
- ⁵A. Erbe, H. Krommer, A. Kraus, R. H. Blick, G. Corso, and K. Richter, *Appl. Phys. Lett.* **77**, 3102 (2000).
- ⁶I. Mahboob and H. Yamaguchi, *Nat. Nanotechnol.* **3**, 275 (2008).
- ⁷D. N. Guerra, M. Imboden, and P. Mohanty, *Appl. Phys. Lett.* **93**, 033515 (2008).
- ⁸D. S. Greywall, B. Yurke, P. A. Busch, A. N. Pargellis, and R. L. Willett, *Phys. Rev. Lett.* **72**, 2992 (1994).
- ⁹R. Almog, S. Zaitsev, O. Shtempluck, and E. Buks, *Appl. Phys. Lett.* **90**, 013508 (2007).
- ¹⁰R. L. Badzey and P. Mohanty, *Nature (London)* **437**, 995 (2005).
- ¹¹I. Siddiqi, R. Vijay, F. Pierre, C. M. Wilson, M. Metcalfe, C. Rigetti, L. Frunzio, and M. H. Devoret, *Phys. Rev. Lett.* **93**, 207002 (2004).
- ¹²R. Almog, S. Zaitsev, O. Shtempluck, and E. Buks, *Phys. Rev. Lett.* **98**, 078103 (2007).
- ¹³G. Anetsberger, O. Arcizet, Q. P. Unterreithmeier, R. Riviere, A. Schliesser, E. M. Weig, J. P. Kotthaus, and T. J. Kippenberg, *Nat. Phys.* **5**, 909 (2009).
- ¹⁴I. Katz, A. Retzker, R. Straub, and R. Lifshitz, *Phys. Rev. Lett.* **99**, 040404 (2007).
- ¹⁵S. S. Verbridge, H. G. Craighead, and J. M. Parpia, *Appl. Phys. Lett.* **92**, 013112 (2008).
- ¹⁶A. K. Hüttel, G. A. Steele, B. Witkamp, M. Poot, L. P. Kouwenhoven, and H. S. J. van der Zant, *Nano Lett.* **9**, 2547 (2009).
- ¹⁷X. M. Henry Huang, C. A. Zorman, M. Mehregany, and M. L. Roukes, *Nature (London)* **421**, 496 (2003).
- ¹⁸Q. P. Unterreithmeier, E. M. Weig, and J. P. Kotthaus, *Nature (London)* **458**, 1001 (2009).
- ¹⁹S. Schmid, M. Wendlandt, D. Junker, and C. Hierold, *Appl. Phys. Lett.* **89**, 163506 (2006).
- ²⁰Q. P. Unterreithmeier, T. Faust, S. Manus, and J. P. Kotthaus, *Nano Lett.* **10**, 887 (2010).
- ²¹A. H. Nayfeh and D. T. Mook, *Nonlinear Oscillations* (Wiley, New York, 1995).
- ²²B. Ritchie and C. M. Bowden, *Phys. Rev. A* **32**, 2293 (1985).
- ²³F. Brennecke, S. Ritter, T. Donner, and T. Esslinger, *Science* **322**, 235 (2008).